Journal of Geoscience and Environment Protection, 2026, 14(7), 330-353
https://www.scirp.org/journal/gep
ISSN Online: 2327-4344
ISSN Print: 2327-4336

Hydrogeochemical Characterization and Quality Assessment of Groundwater in the Lambussie-Karni District, Ghana

Asare Asante-Annor*, Ebenezer Ansah, Priscilla Efua Baiden, Marion Appiah, Nancy Akolpoka Apuriyuure

Geological Engineering Department, University of Mines and Technology (UMaT), Tarkwa, Ghana
Email: *aasante-annor@umat.edu.gh

How to cite this paper: Asante-Annor, A., Ansah, E., Baiden, P. E., Appiah, M., & Apuriyuure, N. A. (2026). Hydrogeochemical Characterization and Quality Assessment of Groundwater in the Lambussie-Karni District, Ghana. *Journal of Geoscience and Environment Protection, 14,* 330-353.
https://doi.org/10.4236/gep.2026.147019

Received: July 6, 2026
Accepted: July 25, 2026
Published: July 28, 2026

Abstract

Groundwater in the Lambussie-Karni District of northwestern Ghana was investigated to determine its hydrogeochemical characteristics, with emphasis on the processes controlling water chemistry and implications for quality and resource sustainability. Groundwater is the main source of domestic water supply in the Lambussie-Karni District of Ghana, yet its quality is influenced by both natural and human factors. This study assessed the hydrogeochemical characteristics of groundwater in the district using physicochemical data from 16 boreholes. Analytical methods included AquaChem software for graphical representations (Piper and Stiff), Microsoft Excel for Gibbs plot and IBM SPSS for multivariate statistical analyses, such as correlation, cluster, and regression. The results showed that the groundwater is fresh, with pH ranging from neutral to mildly alkaline, and TDS values below the WHO guideline, indicating low mineralisation. Major ions followed the order $Ca^{2+} > Mg^{2+} > Na^{+} > K^{+}$ and $HCO_3^- > Cl^- > SO_4^{2-}$, revealing that the dominant hydrochemical facies is Ca-Mg-HCO_3. Gibbs plots confirmed that water chemistry is primarily controlled by rock-water interaction, with minor contributions from precipitation and anthropogenic activities. Correlation and cluster analyses further highlighted the role of silicate mineral weathering and identified recharge zones characterised by fresh Ca-Mg-HCO_3 water types. Groundwater in the Lambussie-Karni District is undersaturated with respect to carbonate and evaporite minerals (aragonite, calcite, dolomite, gypsum, and halite), as indicated by consistently negative saturation indices. This undersaturation reflects ongoing mineral dissolution processes that contribute to the observed ionic composition, rather than oversaturation or secondary mineral precipitation. Regression analysis identified electrical conductivity as the strongest predictor of TDS, under-

scoring the role of dissolved ions in controlling water quality. Overall, the study concludes that groundwater chemistry in the district is dominantly shaped by geogenic processes, with localised human influence, and provides a scientific basis for sustainable water management in the area.

Keywords

Hydrogeochemical Facies, Lambussie-Karni District, Physicochemical Data, Groundwater Quality, Potential Contamination Sources

1. Introduction

Groundwater is known to be a crucial component of water resources worldwide and serves as an essential support for human survival and development. An increase of the population growth in recent years, has rendered groundwater resources to be increasingly exploited for domestic, industrial and agricultural sectors of many countries (Shiklomanov, 1993; Yuan et al., 2022). Groundwater is proportioned differently across the globe, with 65% being used for drinking water, 20% for animal feeding and farming, and 15% for industrial and mining uses (Nayak et al., 2023). According to Golchin and Moghaddam (2016), the greatest threat to maintaining freshwater supplies that are used to fulfil the needs of the rapidly growing human population is the depletion of the surface and groundwater resources.

The quality of groundwater depends on its geological environment, so the concentration of chemical elements in groundwater plays an important role in the classification and assessment of water quality (Zektser & Everett, 2004; Loh et al., 2020). Groundwater is known to contain a high concentration of dissolved ions, that may cause harm to the physical and chemical conditions of both plant life and soils. The osmotic pressures of affected plants experience a significant decrease, which reduces water flow or transmission through various parts of the plant. The soil may also undergo a significant reduction in permeability as result of weak structure and texture (Nayak et al., 2023).

The evaluation and management of groundwater resources, requires one to have a solid understanding of the hydrogeological and hydrogeochemical properties of the aquifer (Golchin & Moghaddam, 2016). The chemical composition of groundwater is influenced by the combination of anthropogenic and human activities, and this combined factor renders the management of groundwater quite complex (Golchin & Moghaddam, 2016; Yuan et al., 2022). Analysing groundwater chemistry can provide valuable insights to the geological history of aquifers and help in determining its suitability for various purposes which may include agriculture, industrial, and or domestic use. As noted by Golchin and Moghaddam (2016), a thorough hydrogeochemical assessment of groundwater systems typically depends on substantial information concerning the groundwater chemistry. Different hydrogeological conditions lead to distinct hydrogeochemical

characteristics in groundwater (Chen & Gui, 2017; Lalumbe & Kanyerere, 2022). The geochemical processes that occur within groundwater and their interactions with aquifer materials can play a significant role in altering groundwater chemistry during recharge and transport phases (Kumar et al., 2006; Wang et al., 2025; Mostafa et al., 2017; Lalumbe & Kanyerere, 2022).

In the Lambussie-Karni district, groundwater chemistry can be affected by a variety of activities, such as agricultural practices that may involve the use of pesticides and fertilisers, livestock farming, urban development and poor waste disposal and sanitation practices. There is limited research regarding the effects of the hydrogeochemical characteristics of groundwater quality in this district. Hence, this study seeks to investigate the hydrogeochemical characteristics of groundwater in the district. The factors influencing water quality and potential contamination sources will be assessed to determine the suitability of groundwater in the area.

2. Materials and Methods

2.1. Overview of the Study Area

The Lambussie-Karni District is in the north-western region of the Ghana Upper West Region and formed out of the Jirapa-Lambussie District in 2007 through LI 1849. It is accessible by both highway and feeder road network and covers an area of approximately 811.9 km^2, with a longitude of 20˚25" and 20˚24"W and a latitude of 10˚25" and 11˚00"N (Anon, 2013; Asante-Annor et al., 2018). It borders Sissala West in the east, Nandom in the west, Jirapa in the south, and Burkina Faso in the north (**Figure 1**) with Hamile being one of the main border towns, which supports cross-border trade (Akanbang & Abdallah, 2021; Anon, 2013). The district is in the tropical continental zone climatically where the annual mean temperatures are 28˚C and 37˚C. It experiences a unimodal rainfall pattern annually between April and July, with few showers from August to October and a long dry period in the months of October to April. Rainfall is erratic between 800 and 1000 mm/year with occasional effects of drought and floods and has a major effect on ground water recharging (Antwi-Agyei et al., 2021; Mwinkom et al., 2021).

The district is located in the Guinea Savannah ecological zone which is a short grass area, a sparse woody environment and species of the environment that withstand drought conditions like baobab and shea trees. Cover of vegetation is also diminished during the long dry season because of the desiccation of grass and frequent bushfires (Yiridomoh et al., 2024). The topographical aspect is part of the Interior Savannah Plains, which is mostly flat to gently undulating in nature with isolated rocky outcrops and plateau regions (300 to 350 m) around Bangwon, Lambussie, Nabaala, and Billaw, which have the potential of gold mineralisation (Anon, 2013; Tetteh et al., 2025). The drainage in the district is poorly developed hydrologically, the Bugbele stream at Piina being the only large stream, and several smaller tributaries of the Black Volta. The dry season causes the drying up of most water bodies leaving the district without surface water (Asante-Annor et al.,

2018; Agodzo et al., 2023).

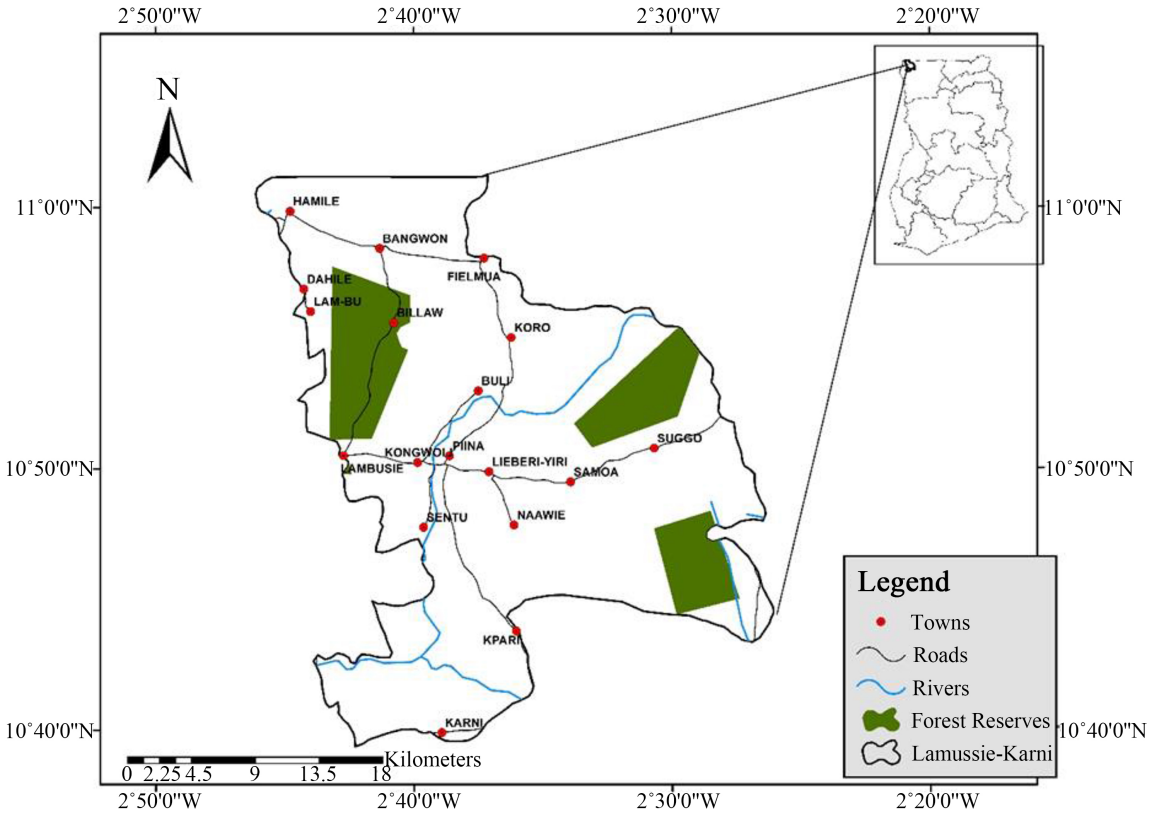

Figure 1. Location map of the study area.

2.2. Geology of the Study Area

The Lambussie-Karni District lies within the northwestern portion of the Birimian Supergroup, part of Ghana's Precambrian basement complex. The area is dominated by Birimian volcanic belts, amphibolites, and plutonic intrusions belonging to the Dixcove and Cape Coast granitoid suites. The Birimian formation has significant granite outcrops around Lambussie, Bangwon, and Billaw (**Figure 2**). These granites serve as important aquifers, storing large amounts of groundwater and supporting the sinking of boreholes and hand-dug wells. The Birimian metavolcanics are mainly composed of meta-basalts and meta-andesites of volcanic and pyroclastic origin, accompanied by two main granitoid types: the Dixcove variety associated with the metavolcanics, and the Cape Coast type, found at the boundary with Birimian sedimentary rocks. Evidence of gold mineralisation occurs in communities such as Lambussie, Bapala East, and Happa, typically hosted in narrow, milky-white quartz veins and streaks within metavolcaniclastics and metasedimentary units. Faults and fissure zones are the key structural features controlling gold mineralisation in the Birimian rocks (Asante-Annor et al., 2018). The numerous faults and fractures that traverse the area acts as conduits for groundwater movement and zones of enhanced water-rock interaction. The dominant rock type in the area is grey phyllite, forming a steeply dipping anticline-

oriented north to north-northwest. The district has mainly sandy loam to clay soils, classified as Savannah Ochrosols and groundwater lateritic intergrades, with Karni in particular characterised by sandy loam soils of low fertility (Offei, 2011).

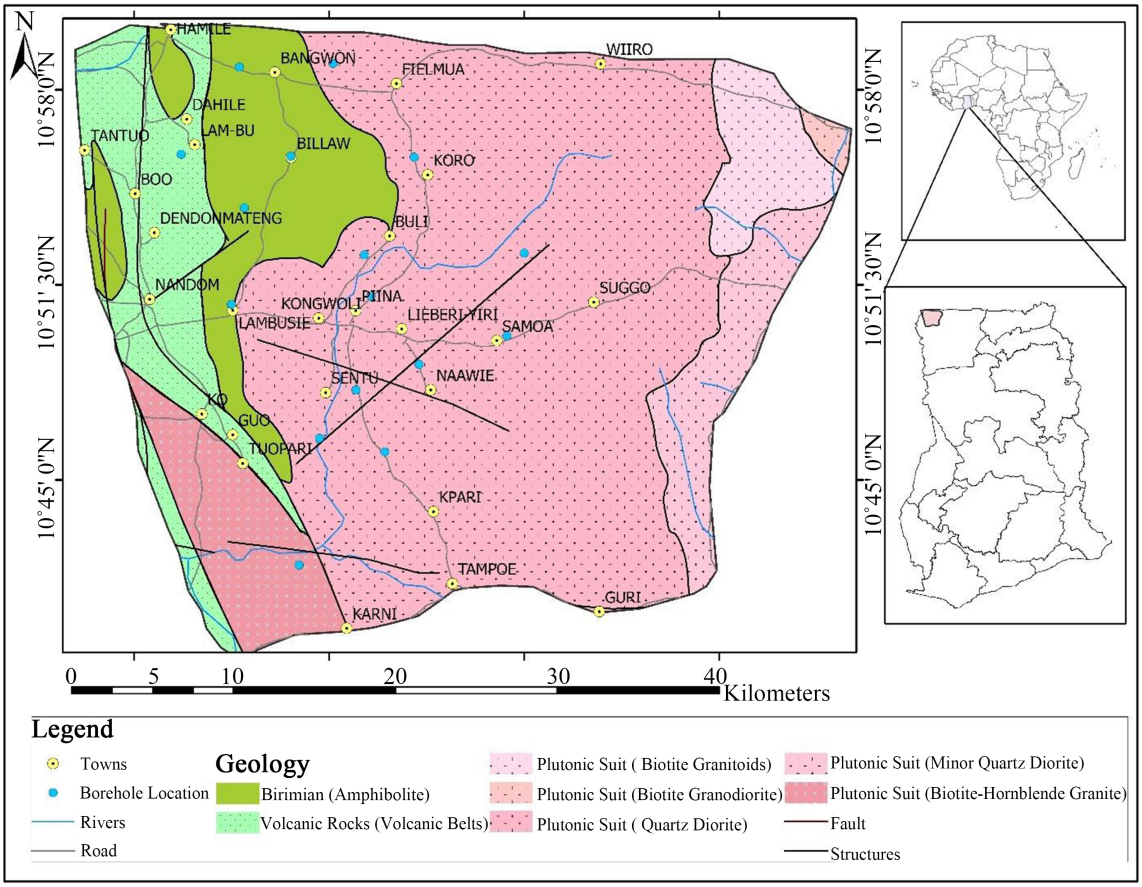

Figure 2. Geological map of the study area.

2.3. Data Acquisition

The information for this study was gathered from previous analyses of physicochemical properties and irrigation water quality in the Lambussie-Karni District. The dataset used in this study was compiled from earlier work on groundwater suitability for irrigation in the Lambussie Karni District of Ghana (Asante-Annor et al., 2018). Given the importance of groundwater as a drinking water source in the area, the dataset was re-evaluated to conduct a hydrogeochemical assessment and identify the factors influencing groundwater chemistry. Groundwater samples were collected in May 2016, during the dry season, thereby representing hydrogeochemical conditions under low recharge and high evaporative influence.

The dataset includes various physicochemical parameters such as pH, Electrical Conductivity (EC), Total Dissolved Solids (TDS) and concentrations of major cations (K^+, Na^+, Ca^{2+}, Mg^{2+}) and anions (Cl^-, SO_4^{2-}, SO_3^{2-} HCO_3^-, NO_3^-, NO_2^-). To ensure consistency in geochemical calculations, all values were reviewed and converted to milliequivalents per litre (meq/L) as required, following standard hy-

drochemical practices outlined by Hem (1985).

The selection of the 16 boreholes, each representing one of the 16 communities in the district was guided by the need to ensure representative coverage of the district's major lithologies, aquifer conditions, and groundwater uses. As shown in **Figure 2**, the boreholes are spatially distributed across the Lambussie Karni District, intersecting the principal geological formations, including the Cape Coast Granite Complex, Undifferentiated Granites, and Birimian Metavolcanic rocks. This distribution allowed sampling across contrasting hydrogeological settings, from fractured crystalline aquifers to weathered metavolcanic zones, thereby capturing variability in groundwater chemistry. The boreholes also reflect the main groundwater use patterns in the district, particularly for domestic supply and irrigation, as they are located near settlements and farming communities. By combining geological diversity with practical water use relevance, the selected boreholes provide a balanced dataset that adequately represents the district's hydrogeochemical conditions and supports robust interpretation of groundwater quality.

Sampling protocols were closely adhered to as established by Barcelona et al. (1985) and Sundaram et al. (2009) throughout the process. Field parameters were measured on-site, while the chemical parameters were analysed in the laboratory at the Water Research Institute (WRI) in Tamale within 24 hours of sampling to ensure the integrity of the samples.

2.4. Data Analysis Techniques

Box and Whisker plot was utilised to show how chemical processes affect the water chemistry in the research area. To classify and visualise the chemical dataset, AquaChem was employed through Stiff Diagram and the hydrogeological facies of the groundwater was determined through Piper/Trilinear Diagram. IBM SPSS 27.0.1 software was used for correlation assessment, hierarchical cluster and multiple linear regression analysis on the data of water quality. The criteria for water quality were primarily based on the World Health Organisation (WHO) guidelines. The influencing factors of hydrochemical characteristics were determined through Gibbs diagram using Microsoft (MS) Excel. Pearson's correlation coefficient (r) was computed to evaluate relationships between physicochemical parameters. For example, a strong positive correlation between EC and Na^+ or Cl^- suggests that salinity is controlled by halite dissolution or evaporative concentration (Hem, 1985).

The correlation function is given as follows:

$$r = \frac{\sum(x1-\bar{x})(y1-\bar{y})}{\sum\sqrt{(xi-x)^2\,(yi-y)^2}} \quad (1)$$

where: r = Pearson correlation coefficient; xi = Values of the x-variable; $\bar{x}$ = Mean of the values of the x-variable; yi = Value of the y-variable; $\bar{y}$ = Mean of the values of the y-variable.

The Saturation Index (SI) for common minerals such as calcite, dolomite, gypsum and halite were calculated using PHREEQC Interactive 3.8.7-17149. This approach assesses whether the water is likely to dissolve or precipitate specific minerals (Appelo & Postma, 2005). The results were then presented using a Q-Q plot to assess whether the dataset is likely of a specific distribution (i.e. linear or non-linear distribution). The Saturation Index was calculated as:

$$SI = \log(IAP/Ksp) \quad (2)$$

In the formula, Ksp represents the dissolution factor at a specific temperature; IAP denotes the ionic strength of the solution; SI > 0 implies mineral oversaturation (potential precipitation); SI < 0 suggests undersaturation (potential dissolution); SI = 0 indicates equilibrium.

2.5. Data Quality Assurance and Charge Balance Error

Table 1. Ionic charge balance error of groundwater.

Town	Σ Cations (meq/L)	Σ Anions (meq/L)	CBE (%)
Ngangor	5	5.03	−0.3
Sina	4.5	4.56	−0.7
Naawie	1.36	1.44	−2.9
Billaw	3.09	3.14	−0.8
Happa	3.94	4.02	−1.0
Hineteng	2.77	2.8	−0.5
Somoa	2.07	2.12	−1.2
Lambuu	4.34	4.4	−0.7
Lambussie	2.22	2.28	−1.3
Tapummu	2.14	2.18	−0.9
Piina	2.55	2.6	−1.0
Hachangan	2.73	2.78	−0.9
Zumura	4.64	4.7	−0.6
Nyambul	2.73	2.78	−0.9
Kpare	2.14	2.18	−0.9
Tabiere	4.62	4.68	−0.6

All laboratory analyses adhered to strict QA/QC protocols, following internationally recognized standards described by Barcelona et al. (1985) and Sundaram et al. (2009). Calibration standards, blanks, and duplicate samples were employed to verify instrument accuracy and precision. The ionic charge balance error (CBE) was calculated for all 16 groundwater samples from the various towns (**Table 1**). A scatter plot shows that the points cluster tightly around the 1:1 line, which confirms that the ionic balance is consistent and the analytical data are reliable (**Figure 3**). Results showed that all samples fell within the acceptable threshold of ±5%,

with a mean error of approximately –1.0%, confirming good analytical quality and reliable ionic balance. This validation step demonstrates that the dataset is robust and suitable for hydrogeochemical interpretation. By adhering to established international laboratory protocols and confirming acceptable charge balance error, the study provides confidence in the accuracy of the groundwater chemistry data used for facies classification and evaluation of mineral controls.

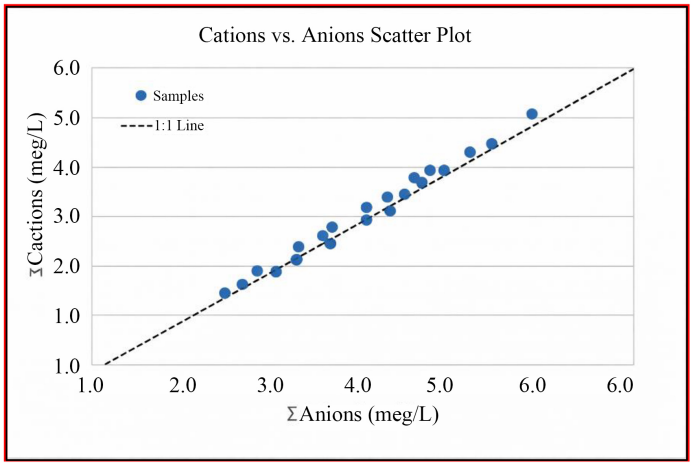

Figure 3. A scatter plot of cations and anions.

3. Results and Discussions

3.1. Results of Geochemical Data

Table 2 presents the descriptive statistics of the physicochemical parameters analysed. These results were assessed against WHO standards. The distribution of most of the parameters in the district is highly variable, suggesting that diverse processes control these parameters in the district. The pH of the water samples ranged from 6.97 to 7.90, indicating that the water was neutral to mildly alkaline. Electrical conductivity is used to detect the concentration of dissolved ions; as EC rises, the concentration of dissolved ions also increases. The EC values ranged between 130 µS/cm and 495 µS/cm, with an average of 296.44 µS/cm. Total Dissolved Solids (TDS) varied from 80.29 to 306 mg/L, with a mean of 183.33 mg/L. The groundwater in the area can be considered fresh due to its low TDS contents. TDS are normally high at areas of discharge, which happens after the water has passed through the rock and dissolved more materials along its flow path, and lowest at points of infiltration, also known as recharge zones. There are more electrolytes and ions accessible in the groundwater systems as a result of more minerals being dissolved by water, which raises EC values. The high values and extreme outliers in EC values are attributable to the influence of the geology and/or impacts of anthropogenic activities which vary widely in space (Chegbeleh et al., 2020).

Sodium ion (Na^+) concentrations ranged from 0.287 to 1.457 meq/L, with an average of 0.63 meq/L. Potassium (K^+) levels ranged from 0.023 to 0.156 meq/L, averaging 0.085 meq/L. Calcium (Ca^{2+}) concentrations were between 0.48 and

3.53 meq/L, with a mean of 1.84 meq/L, while magnesium (Mg^{2+}) ranged from 0.32 to 2.28 meq/L and averaged 1.34 meq/L. Chloride ions (Cl^{-}) ranged from 0.09 to 0.31 meq/L, with a mean concentration of 0.20 meq/L. Bicarbonate (HCO_3^-) levels were between 1.44 and 5.92 meq/L, the concentration of bicarbonate rose at high pH values and decreased at low pH values, indicating a positive relationship with pH. Sulphate (SO_4^{2-}) ranged from 0 to 0.381 meq/L, with an average of 0.068 meq/L, while sulphide (SO_3^{2-}) levels varied from 0 to 0.012 meq/L. The low SO_4^{2-} values may indicate that the region is recharged mostly by HCO_3^-. The SO_4^{2-} values may originate from a mix of man-made activities, such as the use of agrochemicals on farms and ion exchange processes. Nitrate (NO_3^-) concentrations ranged from 0 to 0.11 meq/L, with a mean of 0.03 meq/L, and nitrite (NO_2^-) varied from 0 to 0.003 meq/L, averaging 0.001 meq/L. In terms of mean concentrations (meq/L), the cations followed the order: $Ca^{2+} > Mg^{2+} > Na^+ > K^+ > NH_4^+$, and the anions followed: $HCO_3^- > Cl^- > SO_4^{2-} > SO_3^{2-} > NO_3^-$. Ammonium ($NH_4^+$) was below the detection limit of 0.001 meq/L in most samples, except in Hachangan (0.028 mg/L) and Kpare (0.07 mg/L).

Table 2. Descriptive statistics of the physiochemical parameters.

Parameter	Units	Min	Max	Mean	Median	S.D.	WHO
Conductivity	µS/cm	130.00	495.00	296.44	278.00	133.87	2500
pH		6.97	7.90	7.40	7.39	0.29	6.50 - 8.50
TDS	mg/L	80.29	306.00	183.33	172.50	82.83	1000
NO_3^-	mg/L	1.30	6.50	2.18	1.80	1.30	50
NO_2^-	mg/L	0.004	0.135	0.05	0.04	0.03	N/A
SO_4^{2-}	mg/L	1.70	18.30	6.51	3.50	6.27	400
SO_3^{2-}	mg/L	0.002	0.46	0.12	0.06	0.14	N/A
Ca^{2+}	mg/L	9.62	70.60	36.62	33.6	17.90	200
Cl^-	mg/L	2.98	10.70	6.84	6.46	2.54	250
Mg^{2+}	mg/L	3.87	27.30	16.09	15.45	7.94	150
K^+	mg/L	0.90	6.10	3.31	3.20	1.51	30
Na^+	mg/L	6.60	33.50	14.5	13.25	6.63	200
HCO_3^-	mg/L	87.6	361.00	219.6	195.00	93.27	N/A

3.2. Box and Whisker Plot

The box and whisker plot is also an effective statistical tool which shows how chemical factors are affecting the chemistry of the water in the research area. It shows the data distribution's median, range and shape. The vertical line runs from the minimum to the highest values, and the central box shows the values from the lower to higher quartile (25^{th} to 75th percentile). The diagram clearly shows how the ions Na^+, Ca^{2+}, K^+, Cl^-, Mg^{2+} and HCO_3^- are affected by weathering and human activity. In Figure 4, it can be observed that HCO_3^-, Ca^{2+}, Mg^{2+} and Na^+

highly affect the chemistry of the groundwater in the study area.

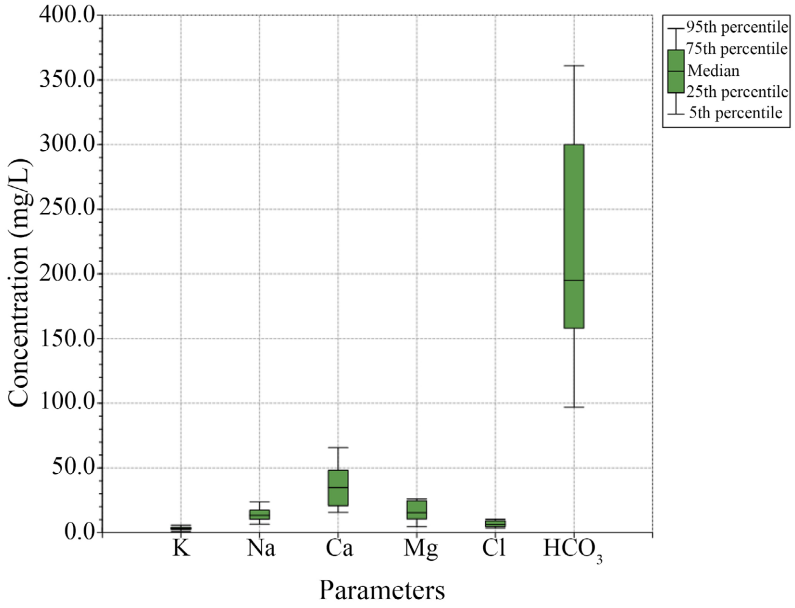

Figure 4. Box and whisker plot of major ions analysed in the groundwater.

3.3. Hydrogeochemical Facies

The hydrogeochemical facies of the groundwater samples analysed in the study area was determined using the trilinear/piper plot. In the cation triangle, groundwater cations (75%) are concentrated mainly in the neutral region, with about four (25%) samples falling in the Ca-rich region which signifies a no dominant type to Ca-rich type. In the anion triangle, the anions (100%) are clustered around the $HCO_3^- + CO_3^{2-}$ region which shows bicarbonate as the dominant anion in the groundwater (**Figure 5**). However, the diagram further suggests the presence of chloride and sulphate water types at very low levels. From the trilinear diagram, the hydrogeochemical facies of the study area is Ca-Mg-HCO_3 with the groundwater being a fresh water type dominated by bicarbonate (HCO_3^-). The percentages of the water types are;

1) Ca-Mg-HCO_3: 56.25%
2) Ca-HCO_3: 6.25%
3) Na-Ca-Mg-HCO_3: 6.25%
4) Ca-Mg-Na-HCO_3: 12.5%
5) Ca-Na-HCO_3: 6.25%
6) Mg-Ca-HCO_3: 6.25%
7) Mg-Ca-Na-HCO_3: 6.25%

The four plots show distinct shapes, **Figure 6(A)** shows a wider shape, with a more pronounced left side. The dominant cation is Calcium (Ca), but the contribution of Magnesium (Mg) is more significant, as indicated by its longer bar. The dominant anion is Bicarbonate (HCO_3^-) with the contributions of Chloride (Cl^-) and Sulphate (SO_4^{2-}) remaining minor. This represents a Ca-Mg-HCO_3 water

type. In a granitic basement terrain like Lambussie-Karni, the Ca-Mg-HCO_3 signature indicates inconsistent hydrolysis of Ca-plagioclase and mafic accessory minerals (biotite, hornblende) by carbon-dioxide (CO_2) charged infiltrating water rather than carbonate dissolution. In contrast to shallower recharge samples, the relatively balanced Ca-Mg contribution indicates that these samples have undergone slightly longer water-rock interaction, likely deeper circulation along fracture networks or weathered zones allowing for a more complete breakdown of both the Ca-bearing plagioclase and the Mg-bearing ferromagnesian minerals (biotite, hornblende).

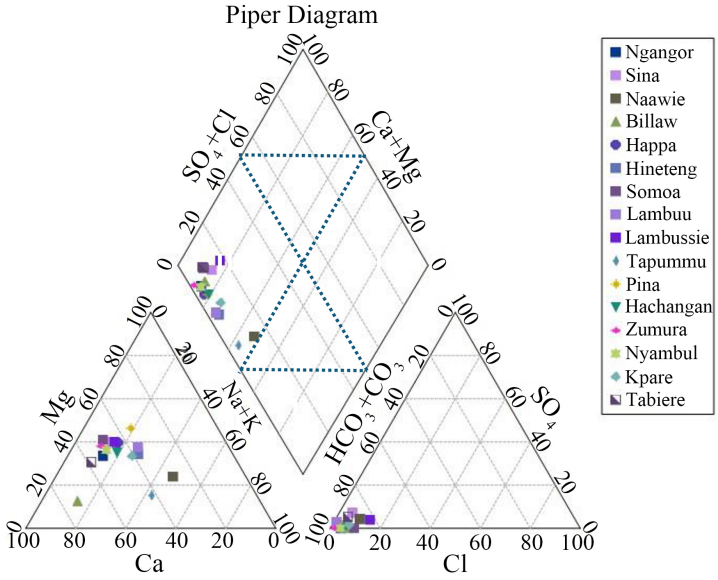

Figure 5. Piper diagram of groundwater.

Figure 6(B) shows a strong symmetrical diamond shape centered around the vertical axis with Calcium (Ca) clearly the dominant cation as indicated by the long bar extending furthest to the left. The dominant anion is Bicarbonate (HCO_3^-), with a bar extending far to the right. It represents a Ca-HCO_3 water type. These facies are very common in recharge areas and shallow groundwater systems that has undergone a carbonation reaction with plagioclase feldspar (the principal Ca-bearing mineral in granite) producing Ca^{2+} and HCO_3^- in near stoichiometric proportions. Rather than deep circulation through the fractured basement, the short symmetrical shape (little Mg, Na, Cl, or SO_4) suggests minimal contribution from the slower-weathering mafic minerals (biotite, hornblende) or K-feldspar which is consistent with a short residence time and shallow, actively recharging groundwater near intake areas.

Figure 6(C) has a very broad, irregular shape, particularly on the cation side with both Calcium (Ca) and Sodium (Na) as significant cation contributors while the dominant anion remains Bicarbonate (HCO_3). It can be classified as a Ca-Na-HCO_3 water type. These facies could be related to the progressive weathering of both plagioclase (releasing Ca^{2+}) and alkali feldspar (releasing Na^+) as water flows

along a longer path or through a thicker weathered layer (saprolite/regolith) overlying the fresh granite. With increasing residence time as infiltrating water interacts with the weathered zone, cation exchange on newly formed clay minerals (kaolinite, illite) can enrich the water in Na^+ relative to Ca^{2+} that gets adsorbed onto clay surfaces.

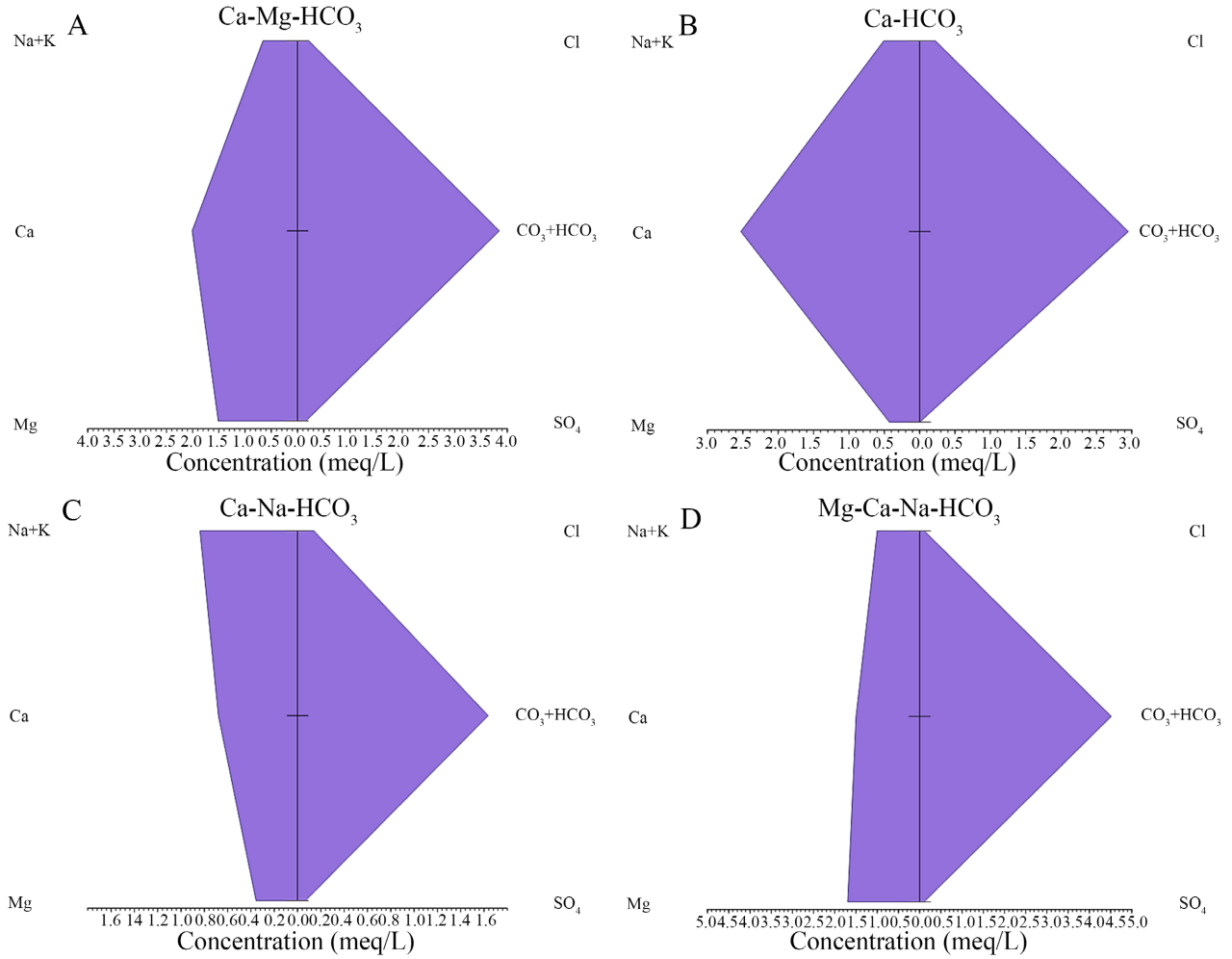

Figure 6. (A) Ca-Mg-HCO_3 Water Type, (B) Ca- HCO_3 Water Type, (C) Ca-Na-HCO_3 Water Type and (D) Mg-Ca-Na-HCO_3 Water Type.

Figure 6(D) has a very broad, irregular shape, particularly on the cation side with Calcium (Ca), Magnesium (Mg) and Sodium (Na), all being significant cation contributors. The dominant anion still remains Bicarbonate (HCO_3). This represents a mixed and more complex hydrogeochemical environment than the other plots and can be classified as a Mg-Ca-Na-HCO_3 water type. These facies could develop due to several processes such as a longer residence time, allowing for more extensive water-rock interaction, including the dissolution of silicate minerals like plagioclase and K-feldspar (releasing Ca, Na), biotite and hornblende (releasing Mg, Ca, K), and subsequent clay-cation exchange (further Na enrichment). It could also represent deeper circulation through fracture zones in

the basement where prolonged residence time allows near-complete hydrolysis of the primary silicate minerals and/or a mixing of a fresher, shallow Ca-HCO_3 recharge water with a more evolved or deeper groundwater that has picked up Mg^{2+} and Na^+ from more extensive silicate weathering along its flow path.

3.4. Gibbs Plot

The Gibbs log plot in Figure 7 represented the ratios of $Na^+/(Na^+ + Ca^{2+})$ and $Cl^-/(Cl^- + HCO_3^-)$ versus TDS, which have been widely applied to study hydrogeochemistry. The Gibbs diagram indicates that the main ions in the groundwater of the district, results mainly from the interaction of groundwater and rock/soil material as compared to other sources such as precipitation and evaporation. However, some water sample in the Gibbs diagram show the predominance of precipitation influencing the hydrochemistry in these portions of the district. This reinforces the assertion that these areas are mainly recharge zones dominated by fresh water types of meteoric origin. Figure 7 does not necessarily imply the absence of the impacts of evaporation on groundwater chemistry. However, suggests that evaporation does not significantly influence most of the major ions in groundwater across the district as compared to the other two factors based on the Gibbs diagram. Another section of the sampling points was distributed outside the Gibbs Diagram, which indicated that the groundwater in the study area was affected by Anthropogenic factor to some extent (Yuan et al., 2022).

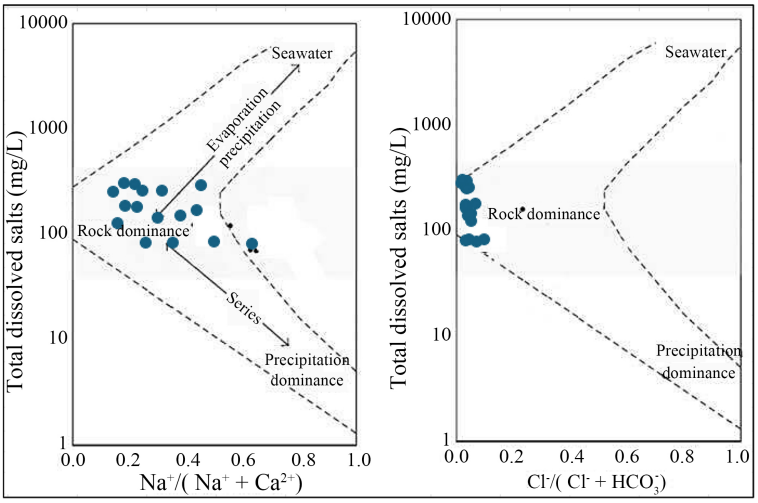

Figure 7. Gibbs Plot of $Na^+/(Na^+ + Ca^{2+})$ and $Cl^-/(Cl^- + HCO_3^-)$ versus TDS.

3.5. Controls on Groundwater Chemistry

3.5.1. Pearson's Correlation Coefficients

Correlation coefficients for the examined parameters were computed to establish a foundation for drawing specific conclusions and identifying relationships between variables, while also enabling the prediction of parameter values at unmeasured locations to a considerable degree. The Pearson correlation coefficient (r) spans from −1 to 1, with −1 representing perfect negative correlation and 1 indi-

cating perfect positive correlation. Table 3 offers a streamlined approach for recognising patterns within water quality variables. Variables exhibiting correlation coefficients (r) of 0.5 or higher are deemed significantly correlated. The relationship between TDS and EC demonstrated a coefficient of 0.99, revealing an ideal positive linear association between these variables. This indicates that TDS has a direct influence on water's electrical conductivity, with EC rising due to elevated ionic concentrations.

Additionally, EC may serve as a substitute measure for TDS. pH exhibited substantial positive correlations with TDS, Ca^{2+}, Mg^{2+}, Na^{+}, and HCO_3^-. Within this group, pH and HCO_3^- displayed the strongest relationship (r = 0.94), with HCO_3^- increasing markedly as pH rises. The positive relationship with pH indicates the potential mobilisation or dissolution of these ions in solutions experiencing pH variations. Bicarbonate demonstrates robust associations with EC, TDS, Ca^{2+}, Mg^{2+}, and Na^{+} (r = 0.94, r = 0.94, r = 0.85, r = 0.93, and r = 0.48, respectively). The pronounced correlation between these cations and HCO_3^- implies a groundwater system potentially characterised by Ca-Mg-HCO_3 freshwater composition, arising from the probable dissolution of carbonate minerals including calcites, dolomites, and aragonite, along with silicate mineral decomposition (Chegbeleh et al., 2020).

Table 3. Pearson's correlation matrix between water quality parameters.

Parameters	EC	pH	TDS	NO_2^-	SO_4^{2-}	SO_3^{2-}	Ca^{2+}	Cl^-	Mg^{2+}	K^+	Na^-	HCO_3^-	NO_3^-
EC	1												
pH	**0.88**	1											
TDS	**0.99**	**0.88**	1										
NO_2^-	−0.02	0.16	−0.02	1									
SO_4^{2-}	0.32	0.09	0.32	−0.24	1								
SO_3^{2-}	0.33	0.07	0.33	−0.29	0.26	1							
Ca^{2+}	**0.82**	**0.73**	**0.82**	−0.12	0.26	0.38	1						
Cl^-	0.1	0.07	0.1	−0.16	0.32	0.04	0.35	1					
Mg^{2+}	**0.91**	**0.84**	**0.91**	−0.02	0.35	0.23	0.7	0.15	1				
K^+	0.08	−0.32	−0.08	−0.09	0.22	0.35	0.22	0.09	−0.25	1			
Na^+	0.44	0.45	0.44	0.18	0.17	−0.18	0.13	−0.47	0.4	−0.23	1		
HCO_3^-	**0.94**	**0.86**	**0.94**	−0.06	0.31	0.28	**0.85**	0.02	**0.93**	−0.09	0.48	1	
NO_3^-	−0.35	−0.19	−0.35	−0.23	0.01	−0.17	−0.16	0.14	−0.29	−0.08	−0.18	−0.29	1

3.5.2. Hierarchical Cluster Analysis

Hierarchical Cluster Analysis (HCA) was applied to groundwater samples from 16 boreholes distributed throughout the district. Based on the dendrogram constructed using Ward's method with Euclidean distance as the similarity metric (Figure 8), the hydrochemical parameters revealed two primary cluster groups,

with the phenon line established at approximately 3.5 linkage distance. In agglomerative schedule cluster analysis, this technique categorises samples into groups according to their distinctive similar properties and mutual associations, positioning the most comparable samples within a single cluster while linking them to closely related cluster(s) and distancing them from clusters with weaker relationships, ultimately connecting all elements to form one comprehensive cluster. The dendrograms clearly illustrate the differentiation among these groups.

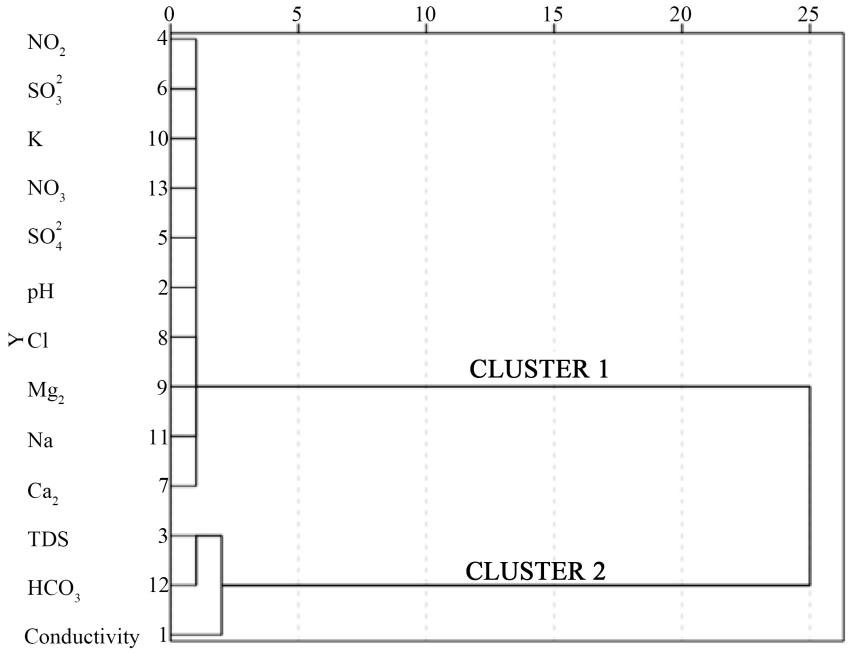

Figure 8. Dendrogram for r-mode cluster analysis.

The parameters are organised into two principal groups. The dendrogram demonstrates strong correlations among TDS, HCO_3, and EC within cluster 2, indicating groundwater dominance by mineral dissolution through substantial water-rock interactions, whereby groundwater reacts with aquifer materials to liberate ions and elevate EC and TDS values. This also indicates associated interaction with atmospheric CO_2. The alternative group, constituting Cluster 1, encompasses Na^+, Cl^-, Ca^{2+}, Mg^{2+}, K^+, SO_4^{2-}, NO_2^-, NO_3^-, SO_3^{2-}, and pH, suggesting potential pollution influences from infiltration, precipitation, and/or recharge processes, likely originating from agricultural fertilizer inputs and associated anthropogenic activities. Agricultural fertilisers, including NKP fertiliser, affect groundwater phosphate, potassium, and nitrate concentrations, as these fertilisers primarily consist of such compounds, while K-rich feldspar weathering contributes to potassium and related ion release into solution. Likewise, sulphate may originate from sulphide mineral oxidation, particularly in recharge zones where aquifer bedrock experiences such exposure conditions. Na^+, Cl^-, Ca^{2+}, Mg^{2+}, and pH may also characterise a groundwater system governed by water-rock interactions, potentially influenced by acidic groundwater environments. This interaction primarily in-

volves bicarbonate and silicate mineral (amphiboles, plagioclase feldspar, pyroxenes and biotite) weathering, which liberates these ions into solution (Chegbeleh et al., 2020).

3.6. Hydrogeochemical Spatial Associations

The Q-mode hierarchical cluster analysis (**Figure 9**) revealed three primary spatial groundwater relationships across the Lambussie-Karni District. These clusters correspond closely with the underlying geological formations and the distribution of borehole locations (**Figure 2**), highlighting the interplay between lithology, hydrogeochemical evolution, and groundwater flow trajectories.

- **Cluster 1 (Lambussie, Tapummu, Naawie, Piina)**

This group is situated predominantly within Birimian volcanic belts and granitoid margins, where shallow recharge zones dominate. The groundwater chemistry here is characterized by relatively low TDS and undersaturation with respect to carbonate minerals, reflecting active carbonate dissolution and silicate weathering. Boreholes in these areas tap aquifers influenced by rapid infiltration and short residence times, consistent with recharge-dominated geochemistry.

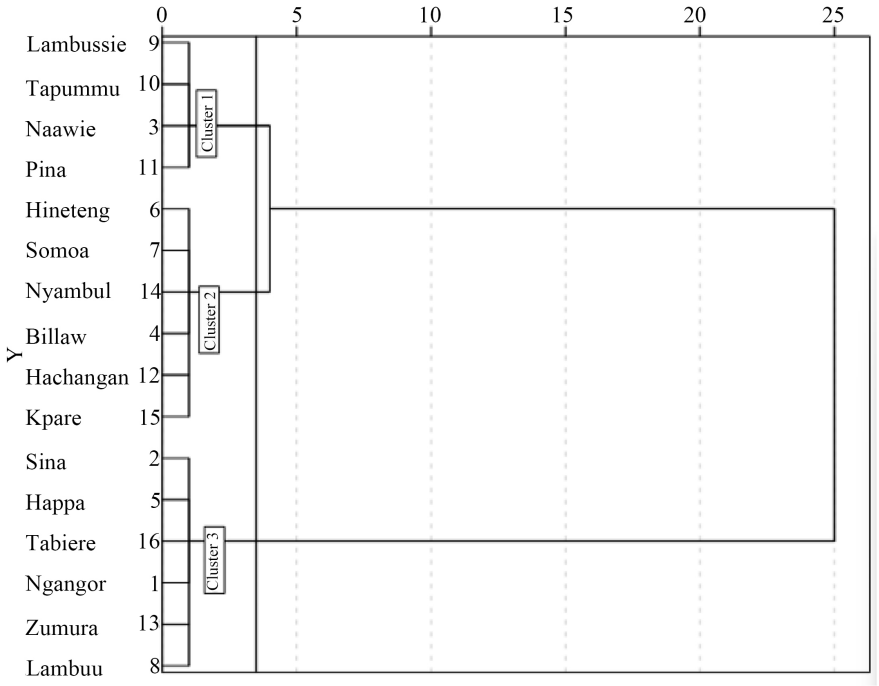

Figure 9. Dendrogram for q-mode cluster analysis.

- **Cluster 2 (Hineteng, Somoa, Nyambul, Billaw)**

These towns lie within mixed granitoid and amphibolite terrains, where intermediate groundwater chemistry is observed. Elevated Ca^{2+} and Mg^{2+} concentrations suggest stronger interaction with calcium plagioclase and mafic mineral phases, while bicarbonate buffering maintains near-neutral pH. Boreholes in this

cluster represent transitional flow zones, where groundwater evolves along intermediate trajectories between recharge and discharge areas.

- **Cluster 3 (Hachangan, Kpare, Sina, Happa, Tabiere, Ngangor, Zumura, Lambuu)**

This cluster corresponds to areas underlain by biotite-hornblende granites and quartz diorites, often located near structural features such as faults and river valleys. Groundwater here shows higher ionic strength and more evolved chemistry, reflecting longer residence times and cumulative water-rock interactions. Boreholes in these discharge-dominated zones capture groundwater that has undergone progressive mineral dissolution, consistent with the undersaturation indices reported for calcite, dolomite, and gypsum.

3.7. Saturation Indices

The saturation index (SI) was defined quantitatively as the deviation of water from equilibrium with respect to the mineral phases and was used to analyse the potential chemical reactions in the groundwater. The values of SI were calculated using the geochemical model PHREEQC Interactive 3.8.7 - 17149.

As shown in Table 4, the SI values for aragonite, calcite, dolomite, gypsum, and halite are consistently negative, with mean values of –4.83, –4.69, –6.35, –8.07, and –11.17 respectively. These negative SI values indicate that groundwater in the Lambussie-Karni District is undersaturated with respect to these mineral phases, meaning that precipitation of secondary carbonates or evaporite minerals is unlikely under the prevailing hydrogeochemical conditions. The negative SI values reflect active mineral dissolution processes, particularly of carbonation reaction with plagioclase feldspar and evaporites, which contribute to the observed ionic composition of groundwater. Thus, the results implied that the dissolution of silicate minerals is the main source of monitored Ca^{2+}, Mg^{2+}, and HCO_3^-. The dissolution of halite may also be responsible for the observed Na^+ and Cl^-, and the dissolution of gypsum was, to a certain extent, the source of Ca^{2+} and SO_4^- of groundwater in the study area. This is consistent with regional studies in crystalline aquifers of Ghana and semi-arid Africa, where undersaturation of calcite and dolomite has been linked to ongoing carbonate, silicate weathering and CO_2-driven dissolution (Apambire et al., 1997; Kortatsi, 2007; Edmunds et al., 2003).

Table 4. Summary statistics of mineral SI of groundwater.

Phase	Minimum	Maximum	Mean	S. deviation
Aragonite	−6.924	−2.202	−4.834	1.827
Calcite	−6.779	−2.058	−4.689	1.827
Dolomite	−8.709	−3.189	−6.351	1.841
Gypsum	−10.797	−5.536	−8.069	1.837

Halite	−12.961	−9.622	−11.168	1.028

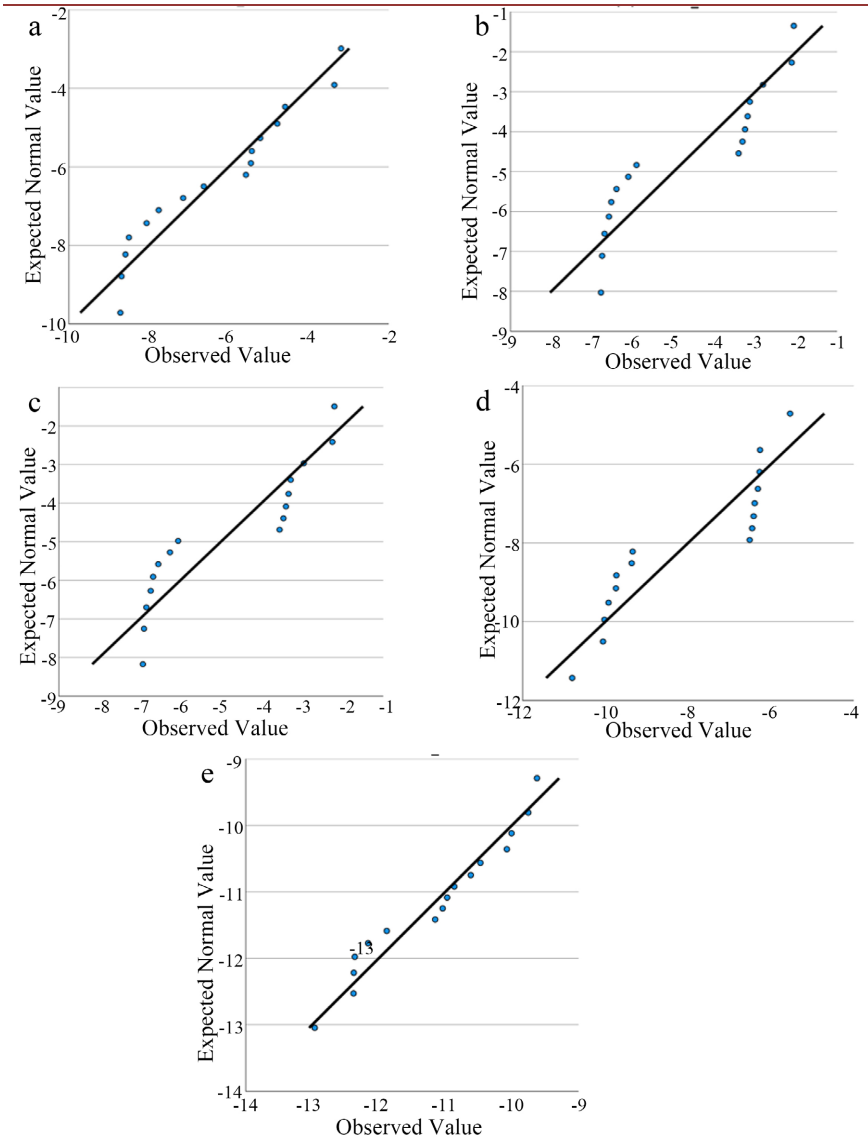

Figure 10. Normal Q-Q Plot of SI of a) Aragonite; b) Calcite; c) Dolomite; d) Gypsum; and e) Halite.

A Q-Q (Quantile-Quantile) plot is a graphical tool used to assess if a set of data is likely to have come from a specific distribution. Plots for Calcite, Aragonite, and Dolomite show a clear non-linear distribution, with the data points deviating significantly from the straight line, particularly at the low and high ends as shown in (**Figures 10(a)-(e)**). This non-normal distribution indicates that the SI values for these carbonate minerals are not clustered around a single mean. Instead, they are influenced by a combination of different conditions or processes. The observed SI values are consistently negative. This is the most crucial finding from these plots, as a negative SI indicates that the water is undersaturated with respect to these minerals, meaning they will tend to dissolve rather than precipi-

tate. The non-normal distribution of the SI values for calcite, aragonite, and dolomite suggests that while dissolution is dominant, the rate and extent of this process vary across different samples. This variation could be due to factors such as differences in water residence time, the partial pressure of carbon dioxide in the soil, or the specific mineralogy of the rocks the water is interacting with. The dominant process controlling the saturation index (SI) values is the dissolution of carbonate and silicate minerals.

3.8. Multiple Linear Regression of Groundwater Chemistry

The multiple linear regression models provide insight into the controls on groundwater chemistry in the Lambussie-Karni District. For TDS, electrical conductivity (EC) was the only statistically significant predictor ($\beta = 0.982$, $p < 0.001$), whereas the coefficients for Ca^{2+}, Mg^{2+}, Na^{+} and HCO_3^- were not statistically significant ($p > 0.05$). The model however showed excellent explanatory power, accounting for 94% of the variation in TDS ($R^2 = 0.941$; Adjusted $R^2 = 0.910$; $F = 12.6$; $p < 0.001$). The strong predictive relationship between EC and TDS is expected because both parameters reflect the total ionic content of groundwater, indicating that EC serves as a good indicator for dissolved mineralization within the study area. The descriptors and the regression coefficient of this model are presented in Table 5.

Table 5. Linear regression predicting TDS.

Variable	β	*t*-value	Sig.t
Constant	-	1.214	0.245
EC	0.982	9.874	0
Ca^{2+}	−0.021	−1.122	0.282
Mg^{2+}	−0.017	−0.984	0.341
Na^{+}	0.006	0.734	0.478
HCO_3^-	0.028	1.046	0.316
Multiple R		0.970	
R square		0.941	
R Adjusted square		0.910	
Standard error		0.642	
F test statistics		12.6	
Significance		0.000	

For pH, the regression model identified Ca^{2+}, Mg^{2+}, HCO_3^-, and TDS as explanatory variables and was statistically significant overall ($R^2 = 0.780$; Adjusted $R^2 = 0.690$; $F = 6.1$; $p = 0.020$), indicating that these variables collectively explained 78% of the variability in groundwater pH. However, none of the individual regression coefficients were statistically significant at the 5% significance level ($p > 0.05$). This indicates that the observed variation in pH is likely influenced by the com-

bined effects of these hydrochemical variables rather than by any single predictor acting independently. The absence of individually significant predictors may also reflect multicollinearity among groundwater quality variables or the relatively limited sample size, both of which can reduce the statistical significance of individual regression coefficients despite an overall significant model. The descriptors and the regression coefficient of this model are presented in Table 6.

Table 6. Linear regression predicting pH.

Variable	β	*t*-value	Sig.t
Constant	-	10.842	0
Ca^{2+}	1.412	1.876	0.084
Mg^{2+}	1.105	1.642	0.128
HCO_3^-	−1.982	−1.734	0.112
TDS	0.214	1.421	0.178
Multiple R		0.883	
R square		0.780	
R Adjusted square		0.690	
Standard error		0.142	
F test statistics		6.1	
Significance		0.020	

3.9. Regression Analysis and Hydrogeochemical Controls on Groundwater Chemistry

The regression analysis identified electrical conductivity (EC) as the dominant statistical predictor of TDS in the Lambussie-Karni District, reflecting the close relationship between EC and the total dissolved ionic content of groundwater. Although Ca^{2+}, Mg^{2+}, Na^+ and HCO_3^- were included because of their hydrogeochemical relevance, their individual effects were not statistically significant after accounting for EC, suggesting that EC captures much of the variability associated with dissolved ions.

The overall regression model for pH was statistically significant, indicating that groundwater acidity-alkalinity is influenced by the combined effects of dissolved ions rather than any single constituent. While Ca^{2+}, Mg^{2+}, HCO_3^- and TDS were not individually significant predictors, they remain important in groundwater geochemistry through their roles in mineral weathering, carbonate equilibria and buffering processes. Overall, the findings suggest that groundwater chemistry in the study area is primarily governed by water-rock interactions, with mineral dissolution and carbonate buffering collectively influencing groundwater quality.

These findings are consistent with similar hydrogeochemical studies in West Africa and beyond. For example, Apambire et al. (1997) reported that groundwater chemistry in northern Ghana is strongly influenced by silicate weathering and carbonate equilibria. Kortatsi (2007) also highlighted the role of bicarbonate and

calcium in buffering groundwater pH in crystalline aquifers of Ghana. Comparable results were observed by Edmunds et al. (2003) in semi-arid Africa, where groundwater chemistry was shaped by mineral dissolution and evaporative concentration. The present study therefore aligns with the broader hydrogeochemical framework established for crystalline basement aquifers while providing additional evidence for the controls on groundwater chemistry in the Lambussie-Karni District

4. Conclusions

This study evaluated the hydrogeochemical characteristics and controlling mechanisms of groundwater in the Lambussie-Karni District of Ghana using an integrated approach of graphical, thermodynamic, and multivariate statistical methods. The following main conclusions are drawn:

- The groundwater quality and facies in the district is predominantly fresh, characterized by neutral to mildly alkaline pH conditions and low mineralization, with total dissolved solids (TDS) safely below the World Health Organization (WHO) regulatory guidelines for drinking water. The abundance of major ions follows the descending order of $Ca^{2+} > Mg^{2+} > Na^{+} > K^{+}$ for cations and $HCO_3^- > Cl^- > SO_4^{2-}$ for anions. Consequently, the Ca-Mg-HCO_3 water type represents the dominant hydrochemical facies, indicating freshly recharged groundwater systems.
- Hydrogeochemical controlling mechanisms and evolution is predominantly governed by geogenic factors, specifically rock-water interactions driven by the dissolution of carbonate and silicate minerals. This is supported by Gibbs plots and cluster analyses, which successfully delineated prominent recharge zones characterized by low-mineralization water types. Anthropogenic inputs and precipitation play only minor, localized roles in modifying the regional water chemistry.
- Thermodynamic modelling indicates that the groundwater is undersaturated. The negative saturation indices for aragonite, calcite, dolomite, gypsum, and halite confirm that groundwater chemistry in the district is controlled by carbonate and evaporite dissolution, consistent with silicate weathering and CO_2 driven equilibria in fractured crystalline aquifers. These processes explain the dominance of bicarbonate and alkaline earth elements in regulating groundwater quality, and they align with regional hydrogeochemical studies in northern Ghana and semi-arid Africa.
- Multivariate statistical tools verified the structural relationships between dissolved ions. Linear regression analysis identified electrical conductivity (EC) as the most robust predictor of TDS, confirming that bulk mineralization in this aquifer system is predictably driven by the dominant dissolved ions.
- The integration of geology maps, borehole distribution, and cluster analysis demonstrates that groundwater geochemistry in the district is strongly controlled by lithology and flow patterns. Recharge areas in volcanic and granitoid

margins yield dilute, bicarbonate-dominated waters, while discharge areas in granitic terrains produce more mineralized waters with higher ionic strength. The clustering results therefore provide a spatial framework that aligns with the hydrogeochemical processes of dissolution, buffering, and flow evolution, reinforcing the conceptual model of groundwater quality progression from recharge to discharge zones.

Overall, the groundwater resources in the Lambussie-Karni District remain of high quality for domestic supply, securely shielded by baseline geogenic governance. These findings establish a crucial hydrogeochemical baseline that local water authorities can utilize to develop targeted monitoring programs, safeguard vulnerable recharge zones, and ensure long-term, sustainable groundwater management in northern Ghana.

Conflicts of Interest

The authors declare no conflicts of interest regarding the publication of this paper.

References

Agodzo, S. K., Bessah, E., & Nyatuame, M. (2023). A Review of the Water Resources of Ghana in a Changing Climate and Anthropogenic Stresses. *Frontiers in Water, 4,* Article 973825. https://doi.org/10.3389/frwa.2022.973825

Akanbang, B. A. A., & Abdallah, A. I. (2021). Participatory Monitoring and Evaluation in Local Government: A Case Study of Lambussie District, Ghana. *Commonwealth Journal of Local Governance, No. 25,* 40-55. https://doi.org/10.5130/cjlg.vi25.8037

Anon (2013). *2010 Population & Housing Census, Regional Analytical Report-Upper West Region*. https://s3-us-west-2.amazonaws.com/new-ndpc-static1/CACHES/PUBLICATIONS/2019/01/21/2010_PHC_Regional_Analytical_Reports_Upper_West_Region.pdf

Antwi-Agyei, P., Abalo, E. M., Dougill, A. J., & Baffour-Ata, F. (2021). Motivations, Enablers and Barriers to the Adoption of Climate-Smart Agricultural Practices by Smallholder Farmers: Evidence from the Transitional and Savannah Agroecological Zones of Ghana. *Regional Sustainability, 2,* 375-386. https://doi.org/10.1016/j.regsus.2022.01.005

Apambire, W. B., Boyle, D. R., & Michel, F. A. (1997). Geochemistry, Genesis, and Health Implications of Fluoriferous Groundwaters in the Upper Regions of Ghana. *Environmental Geology, 33,* 13-24. https://doi.org/10.1007/s002540050221

Appelo, C. A. J., & Postma, D. (2005). *Geochemistry, Groundwater and Pollution* (2nd ed., p. 672) Taylor and Francis.

Asante-Annor, A., Bewil, P. N., & Boateng, D. (2018). Evaluation of Groundwater Suitability for Irrigation in the Lambussie-Karni District of Ghana. *Ghana Mining Journal, 18,* 9-19. https://doi.org/10.4314/gm.v18i1.2

Barcelona, M. J., Gibb, J. P., Helfrich, J. A., & Garske, E. E. (1985). *Practical Guide for Ground-Water Sampling* (169 p). Robert S. Kerr Environmental Research Laboratory, Office of Research and Development, U.S. Environmental Protection Agency.

Chegbeleh, L. P., Akurugu, B. A., & Yidana, S. M. (2020). Assessment of Groundwater Quality in the Talensi District, Northern Ghana. *The Scientific World Journal, 2020,* Ar-

ticle ID: 8450860. https://doi.org/10.1155/2020/8450860

Chen, S., & Gui, H. (2017). Hydrogeochemical Characteristics of Groundwater in the Coal-Bearing Aquifer of the Wugou Coal Mine, Northern Anhui Province, China. *Applied Water Science, 7,* 1903-1910. https://doi.org/10.1007/s13201-015-0365-0

Edmunds, W. M., Shand, P., Hart, P., & Ward, R. S. (2003). The Natural (Baseline) Quality of Groundwater: A UK Pilot Study. *Science of the Total Environment, 310,* 25-35. https://doi.org/10.1016/s0048-9697(02)00620-4

Golchin, I., & Azhdary Moghaddam, M. (2016). Hydro-Geochemical Characteristics and Groundwater Quality Assessment in Iranshahr Plain Aquifer, Iran. *Environmental Earth Sciences, 75,* Article No, 317. https://doi.org/10.1007/s12665-015-5077-0

Hem, J. D. (1985). *Study and Interpretation of the Chemical Characteristics of Natural Water* (263 p). Department of the Interior, US Geological Survey.

Kortatsi, B. K. (2007). Hydrochemical Framework of Groundwater in the Ankobra Basin, Ghana. *Aquatic Geochemistry, 13,* 41-74. https://doi.org/10.1007/s10498-006-9006-4

Kumar, M., Ramanathan, A., Rao, M. S., & Kumar, B. (2006). Identification and Evaluation of Hydrogeochemical Processes in the Groundwater Environment of Delhi, India. *Environmental Geology, 50,* 1025-1039. https://doi.org/10.1007/s00254-006-0275-4

Lalumbe, L., & Kanyerere, T. (2022). Characterisation of Hydro-Geochemical Processes Influencing Groundwater Quality in Rural Areas: A Case Study of Soutpansberg Region, Limpopo Province, South Africa. *Water, 14,* Article 1972. https://doi.org/10.3390/w14121972

Loh, Y. S. A., Akurugu, B. A., Manu, E., & Aliou, A. S. (2020). Assessment of Groundwater Quality and the Main Controls on Its Hydrochemistry in Some Voltaian and Basement Aquifers, Northern Ghana. *Groundwater for Sustainable Development, 10,* Article 100296.

Mostafa, M. G., Uddin, S. M. H., & Haque, A. B. M. H. (2017). Assessment of Hydro-Geochemistry and Groundwater Quality of Rajshahi City in Bangladesh. *Applied Water Science, 7,* 4663-4671. https://doi.org/10.1007/s13201-017-0629-y

Mwinkom, F. X. K., Damnyag, L., Abugre, S., & Alhassan, S. I. (2021). Factors Influencing Climate Change Adaptation Strategies in North-Western Ghana: Evidence of Farmers in the Black Volta Basin in Upper West Region. *SN Applied Sciences, 3,* Article No. 548. https://doi.org/10.1007/s42452-021-04503-w

Nayak, A., Matta, G., & Uniyal, D. P. (2023). Hydrochemical Characterization of Groundwater Quality Using Chemometric Analysis and Water Quality Indices in the Foothills of Himalayas. *Environment, Development and Sustainability, 25,* 14229-14260. https://doi.org/10.1007/s10668-022-02661-4

Offei, S. (2011). *The Role of NGOs and Local Government in the Socio-Economic Development of Lambussie Karni District, Ghana* (p. 88). Master's Thesis, Linköping University.

Shiklomanov, I. A. (1993). *World Freshwater Resources.* Blackwell.

Sundaram, B., Feitz, A., Caritat, P. D., Plazinska, A., Brodie, R., Coram, J., & Ransley, T. (2009). Groundwater Sampling and Analysis—A Field Guide. *Geoscience Australia Record, 27,* 104.

Tetteh, A. T., Issaka, Y., Dodoo, P., Atugba, B., & Tengnibuor, A. (2025). Assessing the Impact of Ghana's Geology on Gold Mining Using Geospatial Techniques. *Heliyon, 11,* e42921. https://doi.org/10.1016/j.heliyon.2025.e42921

Wang, L., Yang, N., Zhao, Y., & Zhang, Q. (2025). Research on the Features and Driving Factors of Shallow Groundwater Quality in Arid Areas, Northwest China. *Water, 17,* Article

934. https://doi.org/10.3390/w17070934

Yiridomoh, G. Y., Bonye, S. Z., & Derbile, E. K. (2024). Reducing Vulnerability to Climate Change among Millet and Sorghum Farmers in Ghana: Interrogating the Contribution of Climate-Smart Agriculture in Northwestern Ghana. *Frontiers in Sustainable Food Systems, 8,* Article 1357355. https://doi.org/10.3389/fsufs.2024.1357355

Yuan, H., Yang, S., & Wang, B. (2022). Hydrochemistry Characteristics of Groundwater with the Influence of Spatial Variability and Water Flow in Hetao Irrigation District, China. *Environmental Science and Pollution Research, 29,* 71150-71164. https://doi.org/10.1007/s11356-022-20685-1

Zektser, I. S., & Everett, L. G. (2004). *Groundwater Resources of the World and Their Use.* Cambridge University Press.